Thermodynamic Behavior of a Supramolecular System Self-Assembled by Electrostatic Interaction in Aqueous Solution. Results And Theoretical Analysis

Ludovic Jullien,*,† Hervé Cottet,‡ Bertrand Hamelin,† and Alain Jardy‡

Département de Chimie (CNRS UMR 8640), Ecole Normale Supérieure, 24 rue Lhomond, F-75231 Paris Cedex 05, France, and Laboratoire de Chimie Analytique des Processus Industriels (CNRS URA 437), Ecole Supérieure de Physique et de Chimie Industrielles, 10, rue Vauquelin, F-75231 Paris Cedex 05, France

Received: March 15, 1999; In Final Form: October 5, 1999

The acid−base and association properties of oppositely charged cyclodextrins in aqueous solution have been investigated by potentiometry. The experimental thermodynamic constants can be analyzed with a theoretical approach leading to structural data in satisfactory agreement with the crystallographic structures of the parent compounds and previous NMR investigations. The corresponding theory is expected to be helpful for understanding and for predicting the behavior of many supramolecular systems involving charged organic molecules.

Introduction

Drug solubilization, targeting, and delivery are major issues for improving the therapeutic efficiency of medical treatments. Supramolecular capsules were recently suggested to open new opportunities as drug carriers.[1] From that point of view, most self-assembled capsules developed until now suffer from two major drawbacks. In fact the attractive interaction governing the assembly process is most often (i) not compatible with water as a solvent, and (ii) poorly tunable so as to favor drug release at well-defined sites. Among the attractive interactions exhibiting tunable stability in water, electrostatic interaction is appealing. If interacting charges result from ionization of acid−base groups, the extent of association can be modified by pH and ionic strength. We have currently investigated some features of a self-assembled capsule held by electrostatic interaction in aqueous solution. Two series of oppositely charged cyclodextrin (CD) derivatives conceived as models of elementary faces for electrostatic interaction were synthesized.[2] Their strong attractive interaction in aqueous solution at low ionic strength was demonstrated in a preliminary report.[3] Then the association was shown to be a dimerization, and the structure of the corresponding dimer was investigated.[4] The latter information on stoichiometry confirmed that the large association constants did not result from aggregation processes.[5] In the present paper, we report on the acid−base and associative properties of our system. The experimental results are analyzed to extract structural parameters that confirmed the data previously collected by NMR.[4]

In addition to the latter aspect, the present paper addresses the prediction of the standard Gibbs free energies of formation of aggregates held together by noncovalent interactions. Such a goal was identified as a fundamental challenge for the development of noncovalent synthesis.[6] The present investigation suggests that electrostatic interaction is suitable for satisfactorily predicting thermodynamic properties such as acid−base and associative properties. It is thus prone to the rational design of supramolecular systems. First, interactions between ions may involve large energies.[7] Thus electrostatic interactions are expected to dominate all the other interactions that can be consequently often neglected in a first approximation. Moreover, several theories are already available to rationalize the structure of systems governed by electrostatic interaction. Some of these are analytical and calculation-limited, whereas others require the extensive use of large computers. As chemists interested in the theoretical side but also concerned with the synthesis and the physicochemical features of supramolecular assemblies, we examined the former approaches. Their major appeal arises from the limited set of "chemically-speaking" structural data (geometry, characteristic distances, intrinsic pK_a of ionizable groups; vide infra) that is required to essentially account for the entire behavior under different environmental conditions. In the present paper, we discuss the relevant molecular description in our supramolecular capsules held by electrostatic interaction and we show that such analytical approaches can be consistently used to derive their thermodynamic properties. As an illustration, some phase diagrams (stability, charge) are derived. Such diagrams are expected to be helpful for screening possible self-assemblies held by electrostatic interaction for drug delivery or other applications.

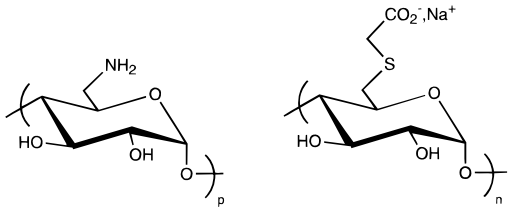

Figure 1. Chemical structures of [CD*p*(Am)] (left; $p = 6$, 7, or 8) and [CD*n*(Ac)] (right; $n = 7$).

Results

The monomers conceived as components for an electrostatically held "press stud" are displayed in Figure 1. They were obtained by introduction of the amino group (positively charged

* To whom correspondence should be addressed. Telefax number: 00 33 (0)1 44 32 33 25. E-mail address: Ludovic.Jullien@ens.fr.
† Ecole Normale Supérieure.
‡ Ecole Supérieure de Physique et de Chimie Industrielles.

10.1021/jp990906v CCC: $18.00
Published on Web 11/19/1999

TABLE 1: Proton Dissociation Constants $-\log K_a(x)$ ($pK_a(x)$) of $[CDp(Am)(H)_p]^{p+}$ ($p = 6$, 7, or 8) and $[CD7(Ac)(H)_7]$ (See Figure 1, Experimental Section, and Text)[a]

x	$[CD6(Am)(H)_6]^{6+}$	$[CD7(Am)(H)_7]^{7+}$ [b]	$[CD8(Am)(H)_8]^{8+}$	$[CD7(Ac)(H)_7]$[b]
1	6.4	6.2	6.4	2
2	7.2	6.8	7.2	3.0
3	7.4	7.3	7.35	4.0
4	8.1	7.6	7.8	4.2
5	8.8	8.4	8.1	5.0
6	9.6	8.9	8.8	5.4
7		9.8	9.0	6.4
8			10.3	

[a] The standard deviation is 0.2 for $pK_a(x)$. [b] The values that are reported for $[CD7(Am)(H)_7](Cl)_7$ and $[CD7(Ac)](H)_7$ herein result from averaging over all the titrations that were performed during the present study. They compare well with the values reported in the previous report,[3] but they are to be considered with more confidence.

series $[CDp(Am)(H)_p](Cl)_p$ ($p = 6$, 7, or 8)) or of the thioglycolic fragment (negatively charged unit $[CDn(Ac)](Na)_n$ ($n = 7$)) on the 6-glucose position of the native cyclodextrins.[2] The notations CDp(Am) and CDn(Ac) are taken to designate the appropriate cyclodextrin backbones bearing no ionizable hydrogen atom (vide infra). In view of their acid−base properties, the CD monomers display different ionization states depending on the pH of the aqueous solution:

$$[CDH_\nu]^{z+} + H_2O = [CDH_{(\nu-1)}]^{(z-1)+} + H_3O^+ \qquad (1)$$

In the preceding reaction, ze is the charge of the cyclodextrin species bearing ν ionizable hydrogen atoms. Hence $z = \nu$ ($\nu \in [1;p]$) in the CDp(Am) series, whereas $z = \nu - n$ ($\nu \in [1;n]$) in the CDn(Ac) series. A priori, such a system can be used for investigating all the types of ionic interactions involving $i+$ and $j-$ charges ($i \in [1;8]$; $j \in [1;7]$). Association constants between the oppositely charged cyclodextrin derivatives were measured by potentiometry as already reported.[3] In a first step, the proton dissociation constants of the monomers were obtained from the titration with sodium hydroxide of their acidified species. The association constants between oppositely charged units were subsequently derived from the simulations of the titration curves of the mixtures.

Potentiometric titrations were first carried out to determine the stepwise proton dissociation constants of the $[CDp(Am)(H)_p]^{p+}$ ($p = 6$, 7, or 8) or $[CDn(Ac)(H)_n]$ ($n = 7$) species. The best simulations resulting from introduction of p or n constants $K_a(x)$ ($x \in [1;p]$ or $x \in [1;n]$) are listed in Table 1.

In a second step, potentiometric titrations of acidified 1:1 and 2:1 CDp(Am):CD7(Ac) mixtures ($p = 6$ or 8) with sodium hydroxide were performed. Their analyses suggested the formation of adducts between CDp(Am) and CD7(Ac) in the ratio 1:1. In view of the structure of the CD7(Am):CD7(Ac) complex,[4] the stoichiometry of these adducts was assumed to be also 1:1. The fit of the experimental points led to the derivation of the thermodynamic constants P_k associated to the formation of the heterodimers $[CDp(Am)CD7(Ac)(H)_k]^{(k-7)+}$ ($k = 1-10$ for $p = 6$, and $k = 1-11$ for $p = 8$)

$$[CDp(Am)(H)_i]^{i+} + [CD7(Ac)(H)_{(7-j)}]^{j-} = [CDp(Am)CD7(Ac)(H)_k]^{(k-7)+} \qquad (2)$$

where $i - j + 7 = k$. In fact, the constants P_k involving k protons are averaged over several constants $P_{i,k}$ which remain individually unknown. As already proposed in the previous report,[3] the constants P_k were taken as corresponding to the association processes involving the maximum number of charges borne by the individual species:[8]

$$[CDp(Am)(H)_i]^{i+} + [CD7(Ac)(H)_{(7-j)}]^{j-} = \{[CDp(Am)(H)_i][CD7(Ac)(H)_{(7-j)}]\}^{(i-j)+} \qquad (3)$$

Table 2 provides the corresponding association constants $\log(P_{ij})$ and standard Gibbs free energies of reaction $\Delta_r G^0_{ij} = -RT \ln(P_{ij})$ that are obtained under the preceding assumption.

Discussion

The discussion is divided into four parts. The first shows that the same theoretical approach can be used for predicting acid−base and association properties in supramolecular systems held by electrostatic interaction. The second part introduces several models for describing the molecular units in the present system. The comparison between the theoretical predictions and the experimental results is discussed in the third part. In the fourth part, the present results are used to derive operational rules for designing supramolecular systems held by electrostatic interaction. In addition, the Supporting Information illustrates how the concepts developed here lead to the devising of phase diagrams for electrostatic interaction in supramolecular systems.

Thermodynamic Analysis of the Problem. The prediction of acid−base properties from molecular structures is an area of continuing interest.[9] As mentioned in the Introduction, we have been most interested in analytical approaches. We eventually concentrated on the work of Tanford and Kirkwood whose theoretical analysis predicts the acid−base properties of any spatial distribution P of ionizable groups.[10] Their theory is based on evaluating the perturbation of the intrinsic acid−base properties that results from the presence of additional charges in close proximity. As will be shown later, the same theoretical frame can be used to rationalize both the dependence on charge and the magnitude of interaction between charged molecules in aqueous solution.

Following Tanford and Kirkwood, one evaluates the standard Gibbs free energies $-RT \ln k_{P(\nu)}$ of the reactions[11]

$$P + \nu H_3O^+ = [P\,H_\nu]^{z+} + \nu H_2O \qquad (4)$$

where P is a spatial distribution of n acid−base groups bearing no ionizable hydrogen atom. Notice that ν and ze, respectively designate the number of ionizable hydrogen atoms and the charge borne on the $[P\,H_\nu]^{z+}$ species. To calculate $k_{P(\nu)}$, one considers a thermodynamic cycle. In a first step, P is discharged (electrostatic work: $-W^0_{P(0)}$), all other things remaining equal. In a second step, one evaluates the standard Gibbs free energy

TABLE 2: Equilibrium Constants log(P_{ij}) and Corresponding Standard Gibbs Free Energies of Reaction $\Delta_r G^0_{ij} = -RT \ln(P_{ij})$ Describing the Association between $[CDp(Am)(H)_i]^{i+}$ and $[CD7(Ac)(H)_{(7-j)}]^{j-}$ at 298 K (See Text and Experimental Section)[a]

$p = 6$			$p = 7$[b]			$p = 8$		
$\|ij\|$	P_{ij}	$-\Delta_r G^0_{ij}$ (kJ·mol^{-1})	$\|ij\|$	P_{ij}	$-\Delta_r G^0_{ij}$ (kJ·mol^{-1})	$\|ij\|$	P_{ij}	$-\Delta_r G^0_{ij}$ (kJ·mol^{-1})
7	4	22.8 (4.0)				7	3.9	22.5 (4.25)
14	4.2	23.4 (4.0)				14	4.6	26.5 (2.55)
21	5.4	31.1 (3.7)	21	4.8	27.35 (8.5)	21	5.3	30.5 (1.7)
28	7.0	39.9 (3.7)	28	5.95	33.9 (8.5)	28	6.1	34.8 (4.0)
35	7.9	45.3 (3.7)	35	7.5	42.75 (5.7)	35	7.4	42.45 (4.0)
42	8.6	49.3 (2.55)	42	9.6	54.7 (4.25)	42	8.6	49.3 (3.7)
36	7.3	41.6 (2.3)	49	11.0	62.7 (2.85)	49	9.4	53.85 (4.85)
30	6.2	35.3 (4.55)	42	8.7	49.6 (4.25)	56	10.0	57.0 (3.15)
24	4.8	27.65 (4.85)	35	7.45	42.45 (5.7)	48	8.4	47.85 (2.3)
18	4.3	24.5 (3.4)				40	6.5	37.4 (2.85)
						32	5.4	31.1 (1.7)

[a] The standard deviation is given in parentheses in kJ·mol^{-1} for $\Delta_r G^0_{ij}$. [b] The present values have been extracted from the titration curves of the previous report[3] by using an improved version of the program TOT.

of the process

$$P\ (\text{uncharged}) + \nu H_3O^+ = [P\ H_\nu]^{z+} + \nu H_2O \qquad (5)$$

It contains two terms: (i) an intrinsic contribution $-\sum_\nu RT \ln k_{int}(P)$ corresponding to the ν bonds that are formed between the P basic sites and the hydrogen atoms originating from the solvated protons, and (ii) the work $\Delta_r G^0_{P(\nu)}$ for charging $[P\ H_\nu]^{z+}$. At that stage, it is important to recognize that the notation $[P\ H_\nu]^{z+}$ considers only one possible distribution of the ν protons over the n basic sites. In fact, at a better level of description, the respective contributions of the $\binom{n}{\nu}$ different configurations indexed by the (k) exponent, $[P\ H_\nu^{(k)}]^{z+}$, have to be taken into account. If $\Omega_\nu^{(k)}$ designates the degeneracy of the $[P\ H_\nu^{(k)}]^{z+}$ configuration and $W_\nu^{0(k)}$ the corresponding charging work

$$\Delta_r G^0_{P(\nu)} = -RT \ln \left[\sum_k \exp\left(- \frac{W_\nu^{0(k)} - RT \ln \Omega_\nu^{(k)}}{RT} \right) \right] \qquad (6)$$

Thus, one has

$$-RT \ln k_{P(\nu)} = -W^0_{P(0)} - \sum_\nu RT \ln k_{int}(P) + \Delta_r G^0_{P(\nu)} \qquad (7)$$

The proton dissociation constants $K_{P(\nu)}$ correspond to the processes

$$[P\ H_\nu]^{z+} + H_2O = [P\ H_{(\nu-1)}]^{(z-1)+} + H_3O^+ \qquad (8)$$

with

$$K_{P(\nu)} = k_{P(\nu-1)}/k_{P(\nu)} \qquad (9)$$

If one links the $K_{P(\nu)}$ to the successive proton dissociation constants $K_a(x)$ ($x \in [1;n]$) classically listed toward the largest values, one obtains the relations $K_a(x) = K_{P(\nu)}$ with $\nu = n + 1 - x$. Then from eqs 7 and 9

$$pK_a(x) = pK_{int}(P) + \frac{1}{\ln 10 RT}(\Delta_r G^0_{P(\nu-1)} - \Delta_r G^0_{P(\nu)}) \qquad (10)$$

$$pK_a(n) = pK_{int}(P) + \frac{1}{\ln 10 RT} W^0_{P(0)} - \frac{1}{\ln 10 RT} \Delta_r G^0_{P(1)} \qquad (11)$$

where $pK_{int} = -pk_{int}$ is expected to aproximate most closely the pK_a in model compounds.

In closer relation to the present system, we now introduce the notations P and N to respectively designate a neutral distribution of p identical amino groups and a n times negatively charged distribution of n identical carboxylic groups (see Figure 1). Then the association process between a i times positively charged species derived from P and a j times negatively charged species derived from N^{n-} gives

$$[PH_i]^{i+} + [NH_{(n-j)}]^{j-} = \{[PH_i][NH_{(n-j)}]\}^{(i-j)+} \qquad (12)$$

The corresponding standard Gibbs free energy $\Delta_r G^0_{ij}$ can be evaluated by considering a thermodynamic cycle involving the acid−base processes represented by eq 4 for the three species $[PH_i]^{i+}$, $[NH_{(n-j)}]^{j-}$, and $\{[PH_i][NH_{(n-j)}]\}^{(i-j)+}$. Hence

$$\Delta_r G^0_{ij} = -RT \ln k_{P(i),N(n-j)} + RT \ln k_{P(i)} + RT \ln k_{N(n-j)} \qquad (13)$$

where the subscript of the k constants denotes the nature and the number of ionizable hydrogen atoms of the considered species. By analogy with eq 7, one has the relation

$$-RT \ln k_{P(i),N(n-j)} = W^0_{P(0),N(0)} - iRT \ln k'_{int}(P) - (n-j)RT \ln k'_{int}(N) + \Delta_r G^0_{P(i)N(n-j)} \qquad (14)$$

where $k'_{int}(P)$ and $k'_{int}(N)$ designate the intrinsic proton dissociation constants of the P amino groups and the N carboxyl groups within the P:N complex. $\Delta_r G^0_{P(i)N(n-j)}$ obeys the general eq 6. If one assumes the absence of major structural modification within P and N accompanying the P:N association,[12] $k'_{int} = k_{int}$ and the k_{int} terms disappear from eq 13. Moreover, if one supposes the degeneracy of the associated species to result only from the proton permutation over the individual P and N species (see eq 6), one has

$$\Omega^{(kk')}_{P(i),N(n-j)} = \Omega^{(k)}_{P(i)} \Omega^{(k')}_{N(n-j)} \qquad (15)$$

where the exponents (k) and (k') respectively denote the distribution of protons within P and N. Eventually, if one additionally writes

$$W^{0(kk')}_{P(i),N(n-j)} = W^{0(k)}_{P(i)} + W^{0(k')}_{N(n-j)} + W^{0(kk')}_{ij} \qquad (16)$$

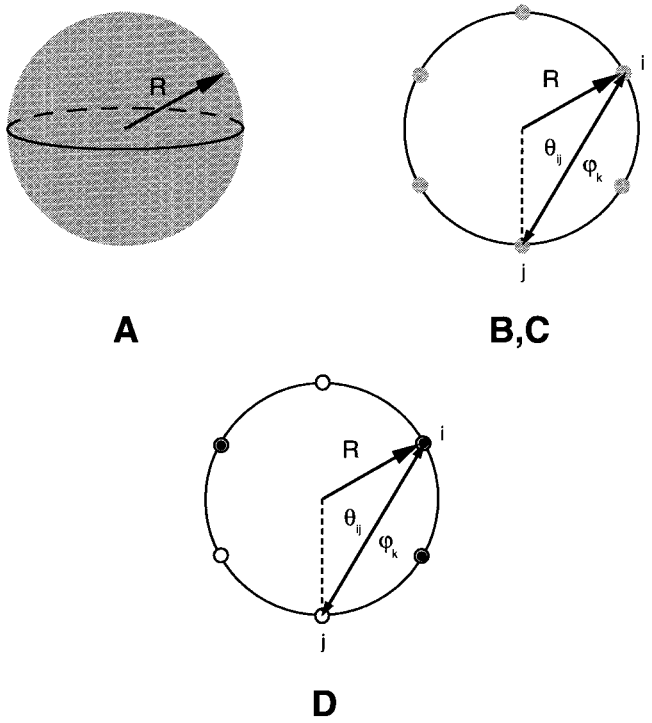

Figure 2. Models A−D used for simulating the acid−base properties of the monomeric cyclodextrins (see text). The charge borne on the CD backbone is either averaged over all the ionizable sites (models A, B, and C; the averaging is associated with the gray color) or not (model D; charged sites in black and neutral sites in white).

eq 13 becomes

$$\Delta_r G^0_{ij} = -W^0_{P(0),N(0)} + W^0_{P(0)} + W^0_{N(0)} - RT \ln \sum_{k,k'} \exp\left(-\frac{W^{0(kk')}_{ij}}{RT}\right) = -RT \ln \sum_{k,k'} \exp\left(-\frac{W^{0(kk')}_{ij}}{RT}\right) \quad (17)$$

since $W^0_{P(0)} = 0$ and $W^0_{P(0),N(0)} \approx W^0_{N(0)}$ in the present system under the assumption that the relative permittivity ϵ_r is identical under all the situations encountered (vide infra).

Equations 6, 10, 11, and 17 show that the evaluation of the acid−base and association properties essentially requires one to estimate the standard chemical potential of charge distributions. This can be done by modeling the charge distributions P and N.

Modeling Interacting Charged Species. To be useful for the audience of synthetic chemists, a model should be as simple as possible as far as the input (introduced set of structural and environmental parameters) and the calculations are concerned. Several models of increasing complexity were chosen for evaluating at which level the description of the charge distribution has to be done for satisfactorily accounting for the properties governed by electrostatic interaction (Figures 2 and 3). The simplest model, denoted A, reduces any charge distribution to its total charge uniformly smeared on a conducting sphere (radius R). The second model, denoted B, takes explicitely into account the geometry of the charge distribution. The CD*p*(Am) and CD*n*(Ac) molecules are now considered as distributions of identical ionizable groups located at the corners of a regular polygon of D_{ph} or D_{nh} symmetry (radius R_p or R_n). In this model, the total charge ze borne on each CD monomer is averaged over its entire backbone. For instance, in the case of nonassociated CD units containing ν ionizable protons: (i) each corner bears the same charge $= \nu e/p$ for CD*p*(Am) and $-(n - \nu)e/n$ for CD*n*(Ac), (ii) the ionizable sites are assumed to be indistinguishable ($\Omega_\nu = 1$), and (iii) the charging work is W^0_ν. Two other models were introduced to account for the acid−base properties of the individual CD units. In contrast to model B, model C considers the ionizable sites as discernible and the global degeneracy $\Omega_\nu = \sum_k \Omega^{(k)}_\nu$ over all the $[PH^{(k)}_\nu]^{z+}$ configurations is taken into account. The charging works W^0_ν are assumed not to depend on (k) and are chosen equal to the charging work W^0_ν from the B model.[13] Eventually the fourth model, D, retains the geometrical description used for models B and C. Nevertheless, the charge is not averaged over the cyclodextrin backbone. Each configuration (ν, k) $[PH^{(k)}_\nu]^{z+}$ is now characterized by a given distribution of the ν protons over the p or n sites with its own $\Omega^{(k)}_\nu$ and $W^{0(k)}_\nu$ values.

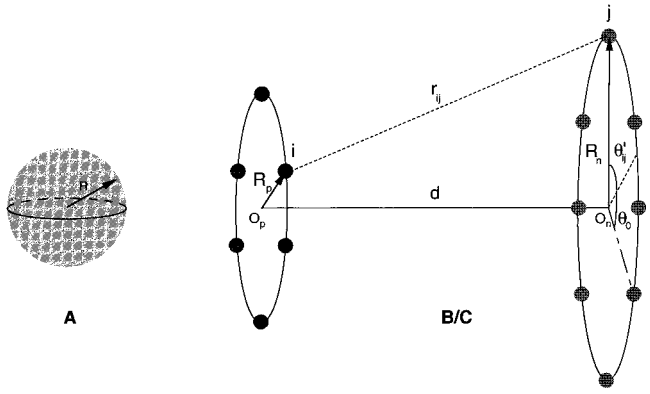

Figure 3. Models A−B/C used for simulating the association properties of the CD*p*(Am):CD*n*(Ac) dimer (see text).

The comparisons between the different models is expected to point out (i) the role of the geometrical description of the charge distribution (A and B), (ii) the significance of taking into account symmetry factors that introduce configurational terms (B and C), and (iii) the consequences of averaging over different configurations (C and D). The calculations leading to the final expressions of the $pK_a(x)$ and $\Delta_r G^0_{ij}$ functions are given in the Appendix for the different models A−D.

Analysis of the Experimental Results. The nature of the constants extracted from potentiometric titrations is first examined. In fact, the mathematical processing of the experimental points provides "apparent" thermodynamic constants K_ν corresponding to eq 1. Indeed, the derived constants K_ν are obtained from iterative calculations where the concentrations are considered to be identical to activities except for the solvated proton whose activity is directly estimated from the pH during the titration. If the infinitely diluted solution at zero ionic strength is taken as the reference system for the cyclodextrin-derived species, K_ν is linked to the "true" thermodynamic constant $K_\nu(I = 0)$ by the relation

$$K_\nu = K_\nu(I = 0)\frac{\gamma_\nu}{\gamma_{(\nu-1)}} \quad (18)$$

γ_ν and $\gamma_{(\nu-1)}$ are, respectively, the activity coefficients of the species containing ν and $(\nu - 1)$ ionizable protons.[14] The theoretical tools developed in the previous paragraphs and in the Appendix evaluate the significant part of the chemical potential for electrostatic interaction at any ionic strength within the limits of validity of the Debye−Hückel theory. Consequently they provide a direct access to the experimentally measured K_ν. They also provide a means to calculate $K_\nu(I = 0)$ since the

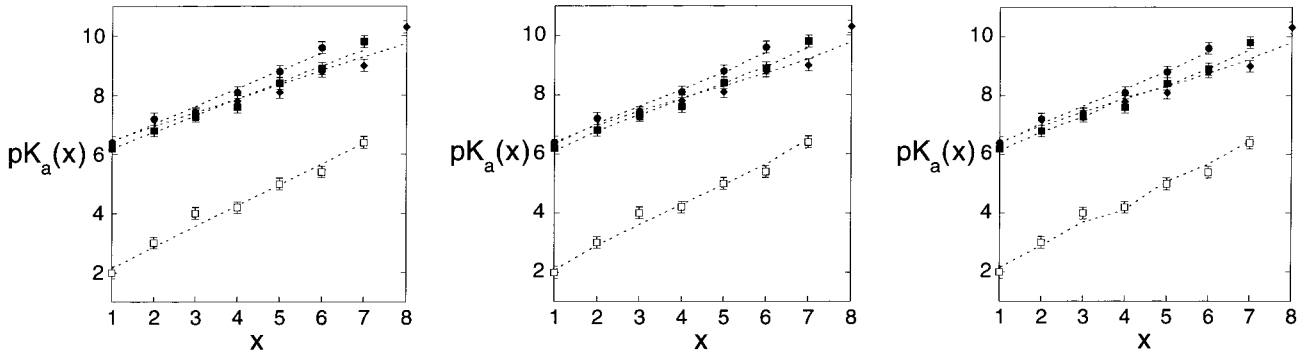

Figure 4. Comparison between the experimental (markers) and the best simulated (dotted lines) proton dissociation constants p$K_a(x)$ for [CDp(Am)] (filled markers; $p = 6$, circles; $p = 7$, squares; $p = 8$, diamonds) and [CDn(Ac)] (empty markers; $n = 7$, squares): (a) left, model A or B; (b) middle, model C; (c) right, model D.

correcting factors can be calculated according to the relation

$$RT \ln \gamma_\nu = -RT \ln \frac{k_{P(\nu)}(I)}{k_{P(\nu)}(I=0)} \tag{19}$$

whose $k_{P(\nu)}$ terms are evaluated from eq 7.

The second issue to be addressed before analyzing the experimental data concerns the values of the parameters present in the equations contained in this paper. The structural description (geometry, size, ...) of the molecular systems and some intrinsic factors such as the intrinsic pK_{int} are the most easily obtained factors, whereas others require a more careful examination. The case of the dielectric constant ϵ_r of the medium and the underlying assumption for all the models A−D that the latter is uniform in solution are first considered. The dielectric constant is the correcting factor for determining charging works in a medium with regard to a vacuum. Such a charging work W is expressed as an integral[15]

$$W = \int_0^{\text{final charge}} \psi(q)\, \mathrm{d}q \tag{20}$$

where ψ is the electrostatic potential created by the body to be charged when it bears the electric charge q. Three points can be made in the present system. First, the electrostatic potential is screened in the frame of the Debye−Hückel theory; the exponential dependence introduces a cutoff in the κ^{-1} range (see eq A7). Under such conditions, eq 20 shows that the charging work is dominated by the polarization work of the water molecules contained within a sphere of radius κ^{-1} centered on the charged body. Thus the final value of the dielectric constant ϵ_r to be used essentially results from the "local" contribution (1 nm < κ^{-1} < 5 nm under the present experimental conditions; vide infra). Second, the external position of the charged groups at the top of short spacers extracts them into the aqueous solution. For the purpose of simplification, this suggests to neglect the discontinuity of the dielectric constant introduced by the presence of the cyclodextrin backbone. Indeed, the hollow cyclodextrin backbone occupies a small solid angle from the charged rim for the calculation of the charging works according to eq 20.[16] Eventually, both the average distance between the charged groups in the charged cyclodextrin derivatives (nanometer range) and κ^{-1} lie much beyond the range where ϵ_r is generally considered to vary around a monovalent ion.[17] In view of such favorable features, we used an empirical approach for deriving an effective uniform dielectric constant instead of (i) assuming a complicated three-dimensional profile for the dielectric constant ϵ_r, (ii) integrating over intercharge distances according to eq 20, and eventually (iii) averaging the resulting value. The present system was considered as a distribution of monovalent ions, and the experimental curve giving the dielectric constant of a NaCl aqueous solution at room temperature was used for calibration. The "local" concentration of ions (ionizable groups and counterions) in a sphere of radius κ^{-1} centered on CDp(Am) or CDn(Ac) was evaluated to lie in the 1−10 M range under our experimental conditions. We then took $\epsilon_r = 50$ since the latter value is representative of the relative permittivity of a NaCl aqueous solution beyond 3 M.[18−20] κ^{-1} was calculated from the Debye−Hückel theory by taking into account the equivalent concentration of monovalent ionic species under the experimental conditions for deriving thermodynamic constants. Eventually, a was taken equal to 0.5 nm in all the calculations (see Appendix).

Analysis of Proton Dissociation Constants. Once ϵ_r, κ^{-1}, and a are defined, the experimental laws p$K_a(x)$ can be used to extract (i) an intrinsic proton dissociation constant connected to the intercept of the p$K_a(x)$ curve with the y-axis and (ii) a characteristic distance to be interpreted as the radius of a sphere (model A) or of a circle (models B, C, and D). The validity of each model is evaluated from the comparison of the extracted values with the expectations based on the pK_a of model compounds or on crystallographic data. In the present system, the rigidity of the cyclodextrin backbone[21] is especially suitable since it prevents any major backbone rearrangement that would lead to a broad range of distances between ionizable groups.

Figure 4 and Table 3 display the results derived from the analysis of the experimental proton dissociation constants with models A−D (see Appendix). All the models satisfactorily account for the essentially linear evolution of p$K_a(x)$ (see R values as calculated from eq 21; Table 3). Models A and B strictly predict a linear behavior (see eqs A3 and A9), whereas model C yields a slight inflection due to the statistical correction (see eqs A13). The present study shows that model D does not introduce a strong deviation from a linear trend. Models A and B yield similar values of the intrinsic proton dissociation constants pK_{int} (9.7−10.1 in the CDp(Am) series and 1.8 for CD7(Ac)). The intrinsic proton dissociation constants extracted from models C and D are also similar (8.7−9.0 in the CDp(Am) series and 2.7−3.0 for CD7(Ac)). Nevertheless they are significantly smaller (CDp(Am) series) and larger (CD7(Ac)) than the corresponding constants obtained from models A and B. The difference is directly related to the correction of configurational entropy made in models C and D. The pK_a of the model compounds 6^A-amino-6^A-deoxy-α- and -β cyclodex-

TABLE 3: Characteristic Radii and Intrinsic pK_a of CDp(Am) (p = 6, 7, or 8) and CDn(Ac) (n = 7) Obtained from the Different Models (see Text)[a]

	CD6(Am)	CD7(Am)	CD8(Am)	CD7(Ac)
		Model A		
$\epsilon_r R_{CD}$ (nm)	21	20	23	14
R_{CD} (nm)	0.42	0.40	0.46	0.28
pK_{int}	9.8	9.8	10.1	1.8
100R	5.0	4.6	7.9	15.4
		Model B		
$\epsilon_r R_{CD}$ (nm)(G_n)	21 (0.50)	25 (0.57)	29 (0.56)	19 (0.55)
R_{CD} (nm)	0.41	0.50	0.58	0.38
pK_{int}	9.7	9.8	10.0	1.8
100R	4.6	4.6	8.0	15.2
		Model C		
$\epsilon_r R_n$ (nm)(G_n)	35 (0.44)	42 (0.52)	51 (0.47)	28 (0.51)
R_n (nm)	0.70	0.84	1.01	0.55
pK_{int}	8.8	8.9	9.0	2.7
100R	4.3	4.2	7.0	12.4
		Model D		
$\epsilon_r R_{CD}$ (nm)	39	49	56	32
R_{CD} (nm)	0.78	0.98	1.11	0.64
pK_{int}	8.7	8.7	8.9	3.0
100R	4.3	5.4	7.1	12.3

[a] The following values of κ^{-1} have been used for the calculations (see text and experimental section): CD6(Am), 2.6 nm; CD7(Am), 4.3 nm; CD8(Am), 3.0 nm; CD7(Ac), 2.6 nm.

trins are already reported to be 8.70 and 8.72, respectively.[22] The latter values compare well with the intrinsic proton dissociation constants extracted from the CDp(Am) data using models C and D so as to support the appropriateness of these models. In contrast to their similarity for deriving the intrinsic pK_{int}, models A and B do not lead to the same characteristic size from interpretation of the pK_a(x) slope. The circle radius arising from model B is larger than the sphere radius obtained from model A. This result is in line with the larger charge delocalization on the sphere surface that affords a smaller radius for a given charging work. For both models A and B, the extracted radii are nevertheless much less than characteristic CD radii (crystallographic diameters of outer periphery:[23] α-CD, 1.46 nm; β-CD, 1.54 nm; γ-CD, 1.75 nm). Model C yields significantly larger values of characteristic radii than models A and B. In the CDp(Am) series, the extracted radii compare well with the expectations based on CPK molecular models by considering that the charged groups point outward owing to the electrostatic repulsion.[4,24] The discrepancy that is observed for CD7(Ac) probably results from the larger hydrophobicity of the spacer with regard to the CDp(Am) series; in CD7(Ac), ϵ_r = 50 is too large an average value giving a too small circle radius R_{CD}. Eventually, model D affords only slightly larger (10−15%) radii than model C. As already suggested from the analysis of the pK_{int}, the structural interpretation of the pK_a(x) slope supports models C and D to be more satisfactory than models A and B for describing the cyclodextrins.

Analysis of Association Constants. Models A and B were used to describe the association between the oppositely charged cyclodextrins. In fact, if one supposes that the protonation states of the interacting units remain unmodified upon association, the configurational terms disappear for evaluating $\Delta_r G^0_{ij}$ (see eq 17). Hence, whereas models B and C are different for predicting the proton dissociation constants, they become identical for describing association. Both models A and B/C predict the standard Gibbs free energy of association $\Delta_r G^0_{ij}$ to linearly depend on the product ij of the charges borne by the individual species (see eqs A5 and A10). Figure 5 displays the experimental $\Delta_r G^0_{ij}(ij)$ relationship. Whereas $\Delta_r G^0_{ij}$ does linearly depend on ij ($-\Delta_r G^0_{ij}$ (kJ·mol^{-1}) = 12.4 + 0.85ij; R = 0.94), it is noticeable that the intercept with the y-axis (−12.4 kJ·mol^{-1}) is not zero as predicted by eqs A5 and A10. This residual attractive contribution probably results from a hydrophobic interaction between the large solvent-destructurating CD backbones. Indeed the experimentally measured distance d between the interacting oppositely charged cyclodextrins ($d \approx$ 0.6 nm;[4] see Figure 3) is too large to invoke any direct contribution such as hydrogen bonding. Since R_p and R_n are derived from the pK_a(x) curves (vide supra), the distance d can be extracted from the slope of the $\Delta_r G^0_{ij}(ij)$ function in the frame of model B/C (Figure 3). The experimental slope (0.85 kJ·mol^{-1}) of the $\Delta_r G^0_{ij}(ij)$ linear function compares well with the values predicted under our experimental conditions where $\kappa^{-1} \approx$ 2 nm (See Appendix and Supporting Information). In fact, the previously reported NMR experiments[4] gave $d \approx$ 0.6 nm. With the latter d value, the predicted slopes S_{p7} are, respectively, 0.93 kJ·mol^{-1} (p = 6), 0.90 kJ·mol^{-1} (p = 7), and 0.82 kJ·mol^{-1} (p = 8). Unfortunately, S_{pn} is a slowly varying function of d (Figure 5Sb). Consequently d cannot be precisely determined from the $\Delta_r G^0_{ij}(ij)$ relationship. Nevertheless the satisfactory agreement between the order of magnitude that is obtained from the $\Delta_r G^0_{ij}(ij)$ correlation and from NMR measurements strongly supports model B/C to be suitable for predicting the stability of the present self-assembled capsule.

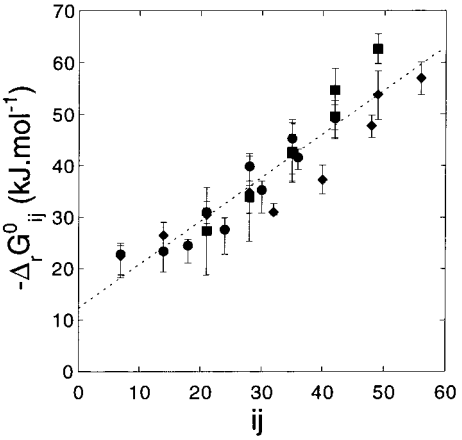

Figure 5. Standard Gibbs free energy $\Delta_r G^0_{ij}$ of ion pair formation between the i times positively charged species from CDp(Am) (p = 6, circles; p = 7, squares; p = 8, diamonds) and the j times negatively charged species from [CDn(Ac)] (n = 7) as a function of ij. The best linear fit (dotted line) of the experimental points gives $-\Delta_r G^0_{ij}$ (kJ·mol^{-1}) = 12.4 + 0.85ij.

Electrostatic Interaction as a Predictive Tool for Self-Assembly. Upon assuming that the self-assembled system is governed by a regime of linear electrostatic screening (large charge−charge distances within and between interacting units, large ionic strength, ...),[25] the present results demonstrate that all the ij pairwise interactions determine the electrostatic interaction within and between charged bodies. Nevertheless, the significance of each elementary (i, j) interaction depends on the value of r_{ij} with regard to κ^{-1}. If $r_{ij} < \kappa^{-1}$, this interaction contributes to the total interaction, whereas if $r_{ij} > \kappa^{-1}$, it does not play any role.[26] This observation bears much significance for designing molecular units in self-assembled systems held by electrostatic interaction. The design has to be "territorial" since charged zones that are distant by more than κ^{-1} will essentially behave independently. Figure 6 provides a guideline for devising supramolecular systems held by electrostatic interaction. Two bodies are designed for assembling by interaction between oppositely charged zones (A, B, and C on one

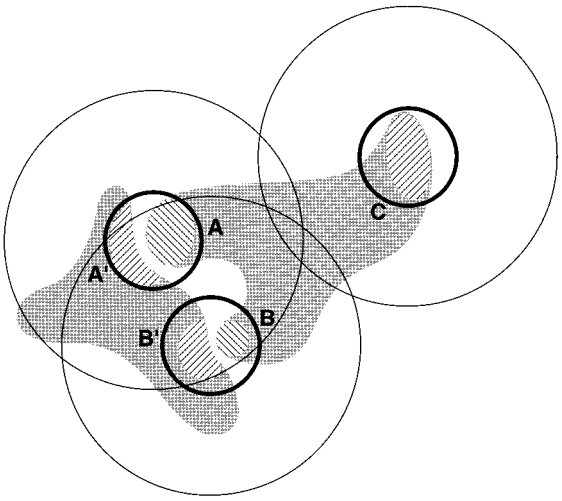

Figure 6. Schematic representation picturing the electrostatic interaction between charged areas borne on molecular units in a supramolecular system. The thin and thick circles (radius: κ^{-1}), respectively, delimitate the range of the electrostatic interaction exerted by each charged zone at low and large ionic strength.

hand and A′, B′ on the other hand). Two different situations are encountered according to κ^{-1}. At low κ^{-1}, the range of the electrostatic interaction displayed as a thick circle in Figure 6 is short. Under such conditions, the different zones A, B, C and A′, B′ are independent. One has only two contributions for association, AA′ and BB′, that are additive. In contrast, at large enough κ^{-1} (thin circles), the charged zones "see" each other within and between each interacting body. The molecular design must include the corresponding cross terms for properly evaluating the final electrostatic interaction. From this point of view, the electrostatic interaction is at the same time more simple and more complicated than the other interactions for the synthetic chemists. Indeed it can be sometimes simply additive without any complication arising from conformational considerations. It may also occasionally involve distant charged groups whose interaction via other sources such as hydrogen bonds should be easily discarded.

Conclusion

The present paper strongly supports that the electrostatic interaction can be used for rationally building noncovalent self-assembled oligomeric arrays in aqueous solution. Thus, the association between oppositely charged cyclodextrin derivatives is shown to provide very stable dimers at low ionic strength. In addition, the acid−base and association constants collected during the present study were used to extract structural data in good agreement with independent structural data available from crystallographic or spectroscopic sources. Hence the comparisons between experimental and predicted thermodynamic constants lead to the conclusion that the prominent features of electrostatic interaction in the present supramolecular system are satisfactorily accounted for by assimilating the charged species to appropriate distributions of charges. After evaluation of several models, the best compromise between simplicity and efficiency consists of (i) modeling the aqueous environment as a continuum of appropriate dielectric constant obtained from a suitable experimental calibration, (ii) accounting for the geometry of the charge distribution that is derived from molecular structures, (iii) averaging the charge borne by the interacting molecules over all the ionizable sites of the individual species, and (iv) taking into account the possible symmetry factors when dealing with acid−base properties. More detailed descriptions involving multiple configurations do not strongly modify the picture emerging from the preceding model so as to justify longer calculations. The present theoretical analysis is meant as a useful operational guideline for designing structurally tunable supramolecular systems from a limited set of easily devisable data as long as these systems are (i) hydrophilic enough and (ii) governed by a regime of linear electrostatic screening (large charge−charge distances within and between interacting units, large ionic strength, ...). The present appealing results are expected to encourage future efforts to be undertaken for building larger and more complex assemblies held by electrostatic interaction for drug delivery and other applications.

Experimental Section

Synthesis. The syntheses of the CD*p*(Am) and CD7(Ac) were already reported elsewhere.[2]

Titrations. The potentiometric titrations were carried out with a Solea-Tacussel TT2 titrimeter, using a glass electrode for high alkalinity and a calomel reference Tacussel. The solutions were prepared from deionized and boiled water flushed with N_2 upon cooling. The 0.05 M NaOH solution was prepared from a Titrisol set and kept free of carbon dioxide. The entire cell was thermostated at 25 °C. A stream of nitrogen, presaturated with water vapor by bubbling, was passed over the surface of the solution. The pH meter was calibrated with a solution of potassium hydrogentartrate at pH = 3.557 at 25 °C and a Tacussel buffer solution at pH = 7.001 at 25 °C. If necessary HCl in 0.1 M aliquots was added to reach low pH to analyze the data in the widest pH range. The following initial solutions were used for the potentiometric measurements: (i) for titration of CD6(Am), 15.1 mg of CD6(Am) in water (5.0 mL), $[CD6(Am)]_0 = 2.28 \times 10^{-3}$ M, analyzed pH range 4.5−11.5; (ii) for titration of CD8(Am), 14.8 mg of CD8(Am) in water (5.0 mL), 0.9 mL of 0.1 M HCl, $[CD8(Am)]_0 = 1.64 \times 10^{-3}$ M, analyzed pH range 2.6−11.5; (iii) for titration of the mixture [CD7(Ac)]/[CD6(Am)] 1/1.02; 7.6 mg of CD6(Am), 10.15 mg of CD7(Ac) in water (5.0 mL), 0.5 mL of 0.1 M HCl, $[CD7(Ac)]_0 = 1.02 \times 10^{-3}$ M, $[CD6(Am)]_0 = 1.04 \times 10^{-3}$ M, analyzed pH range 2.3−11.5; (iv) for titration of the mixture [CD7(Ac)]/[CD6(Am)] 1/2.04, 10.6 mg of CD6(Am), 7.1 mg of CD7(Ac) in water (5.0 mL), 0.5 mL of 0.1 M HCl, $[CD7(Ac)]_0 = 7.2 \times 10^{-4}$ M, $[CD6(Am)]_0 = 1.46 \times 10^{-3}$ M, analyzed pH range 2.2−11.5; (v) for titration of the mixture [CD7(Ac)]/[CD8(Am)] 1/1.05, 9.1 mg of CD8(Am), 10.25 mg of CD7(Ac) in water (5.0 mL), 1 mL of 0.1 M HCl, $[CD7(Ac)]_0 = 9.5 \times 10^{-4}$ M, $[CD8(Am)]_0 = 9.9 \times 10^{-4}$ M, analyzed pH range 2.2−11.5; (vi) for titration of the mixture [CD7(Ac)]/[CD8(Am)] 1/1.76, 11.05 mg of CD8(Am), 7.4 mg of CD7(Ac) in water (5.0 mL), 1 mL of 0.1 M HCl, $[CD7(Ac)]_0 = 6.8 \times 10^{-4}$ M, $[CD8(Am)]_0 = 1.20 \times 10^{-3}$ M, analyzed pH range 2.3−11.5.

The data collected during the titrations were analyzed with the computer program TOT.[27] Each point of simulated curves is calculated by iteration. Once the present acidic and basic species are chosen, proton dissociation and association constants are determined from iterative comparison between simulated curves and experimental points. Uncertainties on constants are estimated from observation of significant deviations between the simulated curves and experimental points after systematic introduction of increments to the constants.

Fitting Process of the Experimental $pK_a^{exp}(x)$. The best fits were obtained from optimization of the factor

$$R = \sqrt{\sum_x \left(\frac{pK_a^{sim}(x) - pK_a^{exp}(x)}{pK_a^{exp}(x)} \right)} \qquad (21)$$

where $pK_a^{sim}(x)$ and $pK_a^{exp}(x)$ respectively designate the simulated $pK_a(x)$ ($\epsilon_r R$ and pK_{int} as floating parameters) and the experimental data given in Table 1.

Appendix. Determination of the Proton Dissociation and Association Constants in the Frame of the Models A−D

Model A. The molar work W_z^0 associated with the process of introducing a charge ze on the surface of a conducting sphere of radius R immersed in a medium of homogeneous dielectric constant is equal to[28]

$$W_z^0 = \frac{N_A z^2 e^2}{8\pi\epsilon_0\epsilon_r}\left(\frac{1}{R} - \frac{\kappa}{1+\kappa a}\right) \qquad (A1)$$

where N_A designates Avogadro's number, κ^{-1} is the Debye−Hückel reciprocal length, e the elementary charge of the proton, ϵ_0 the vacuum permittivity, and ϵ_r the relative permittivity of the aqueous solution. In eq A1, a is a mean distance of closest approach that should be intermediate between the sum of the crystallographic and solvated radii of the ionizable groups borne on the CD and the oppositely charged ion of the supporting salt.[15] In the present system, a should be typically in the 0.5−0.6 nm range.

Since no configurational terms are involved in the model A, eq 6 transforms into

$$\Delta_r G_\nu^0 = W_\nu^0 = W_z^0 = \frac{N_A z^2 e^2}{8\pi\epsilon_0\epsilon_r}\left(\frac{1}{R} - \frac{\kappa}{1+\kappa a}\right) \qquad (A2)$$

with $z = \nu$ and $\nu \in [1;p]$ in the CDp(Am) series, whereas $z = \nu - n$ and $\nu \in [1;n]$ in the CDn(Ac) series. Then eqs 10 and 11 become

CDp(Am) series:

$$pK_a(x) = pK_{int}(\mathrm{Am}) - \frac{N_A e^2 (1+2p)}{8\pi\epsilon_0\epsilon_r RT \ln 10}\left(\frac{1}{R_p} - \frac{\kappa}{1+\kappa a}\right) + \frac{N_A e^2(x)}{4\pi\epsilon_0\epsilon_r RT \ln 10}\left(\frac{1}{R_p} - \frac{\kappa}{1+\kappa a}\right) \qquad (A3.a)$$

CDn(Ac) series:

$$pK_a(x) = pK_{int}(\mathrm{Ac}) - \frac{N_A e^2}{8\pi\epsilon_0\epsilon_r RT \ln 10}\left(\frac{1}{R_n} - \frac{\kappa}{1+\kappa a}\right) + \frac{N_A e^2(x)}{4\pi\epsilon_0\epsilon_r RT \ln 10}\left(\frac{1}{R_n} - \frac{\kappa}{1+\kappa a}\right) \qquad (A3.b)$$

Equation A1 also provides the self-energy of a P(i):N($n-j$) adduct if it is supposed spherical (radius R_{PN}):

$$\Delta_r G^0_{P(i),N(n-j)} = W^0_{P(i),N(n-j)} = \frac{N_A (i-j)^2 e^2}{8\pi\epsilon_0\epsilon_r}\left(\frac{1}{R_{PN}} - \frac{\kappa}{1+\kappa a}\right) \qquad (A4)$$

If one assumes that the species involved in the association process 12 are spherical with the same radius; $R_{CD} = R_p = R_n = R_{PN}$, eqs A2 and A4 transform eq 17 into

$$\Delta_r G_{ij}{}^0 = -\frac{N_A e^2}{4\pi\epsilon_0\epsilon_r}\left(\frac{1}{R_{CD}} - \frac{\kappa}{1+\kappa a}\right) ij \qquad (A5)$$

Model B. The molar work W_ν^0 to place ν protons on the P charge distribution is calculated by summing the terms associated to the electrostatic interactions over all the ij ($i \neq j$) pairs of charged sites (Figures 2 and 3). Furthermore, no configurational terms are involved in the model B so as to give:

$$\Delta_r G_\nu^0 = W_\nu^0 = W_z^0 = \sum_{\substack{(i,j)\\ i\neq j}} \frac{1}{2}\left(\frac{z}{n}\right) e\psi_j = \frac{1}{2}\left(\frac{z}{n}\right)^2 \frac{ne^2 N_A}{4\pi\epsilon_0\epsilon_r R_n} \sum_{j=2}^{n} \frac{e^{\kappa(a-r_{1j})}}{\left(\frac{r_{1j}}{R_n}\right)(1+\kappa a)} = \frac{1}{2}\frac{z^2 e^2 N_A}{4\pi\epsilon_0\epsilon_r R_n} G_n \qquad (A6)$$

To establish eq A6, use was made of the Debye−Hückel theory to derive the relation

$$\psi_j = \frac{z_j e N_A}{4\pi\epsilon_0\epsilon_r} \frac{e^{\kappa(a-r)}}{r(1+\kappa a)} \qquad (A7)$$

giving the electrostatic potential ψ_j at a distance r from a charge $z_j e$ in an electrolytic solution in a regime of linear electrostatic screening.[15,25]

The term

$$G_n = \frac{1}{n}\sum_{j=2}^{n} \frac{\exp[\kappa(a - R_n[2(1-\cos\theta_{ij})]^{1/2})]}{[2(1-\cos\theta_{ij})]^{1/2}(1+\kappa a)} \qquad (A8)$$

with

$$\theta_{ij} = \left(2\pi\frac{(j-1)}{n}\right)$$

is a numerical factor that depends on the geometry of the charge distribution (symmetry D_{nh}, R_n), on the ionic strength I ($\kappa(I)$), and on a. At given R_n, κ^{-1}, and a, G_n logarithmically diverges with n (Figure 4Sa). This behavior is related to the divergence of the self-energy of a charged circle. As expected, G_n increases when n rises (smaller distance between charges) or when the reciprocal Debye length κ^{-1} is increased (less efficient charge screening). At given R_n, n and a, G_n is a logarithmically increasing function of κ^{-1} that then levels off (Figure 4Sb). This two-stage behavior agrees with the two regimes that respectively correspond to (i) $\kappa^{-1} <$ a few R_n—only the closest neighbors determine the self-energy of the charge distribution, and the electrostatic interaction is screened; (ii) $\kappa^{-1} >$ a few R_n—all the charges contained in the polygonal distribution are taken into account, and the electrostatic interaction is essentially not screened anymore. It is interesting to notice that the first regime is poorly sensitive to n, that is, to the cyclodextrin series.

Under consideration that the degeneracy of any charge distribution is equal to one in model B, eqs 10 and 11 become

CD*p*(Am) series:

$$pK_a(x) = pK_{int}(Am) - \frac{N_A e^2 (1+2p) G_p}{8\pi\epsilon_0\epsilon_r RT \ln 10 R_p} + \frac{N_A e^2 G_p}{4\pi\epsilon_0\epsilon_r RT \ln 10 R_p}(x) \quad \text{(A9.a)}$$

CD*n*(Ac) series:

$$pK_a(x) = pK_{int}(Ac) - \frac{N_A e^2 G_n}{8\pi\epsilon_0\epsilon_r RT \ln 10 R_n} + \frac{N_A e^2 G_n}{4\pi\epsilon_0\epsilon_r RT \ln 10 R_n}(x) \quad \text{(A9.b)}$$

The standard Gibbs free energy $\Delta_r G^0_{ij}$ can be similarly evaluated. Since the charges borne by the individual CD*p*(Am) and CD*n*(Ac) are unaffected upon the association 12, only cross terms remain in the evaluation of W_{ij} in eq 16 so as to eventually give

$$\Delta_r G^0_{ij} = \sum_{i,\mathrm{CD}p(\mathrm{Am})} \sum_{j,\mathrm{CD}n(\mathrm{Ac})} \left(\frac{i}{p}\right)\left(\frac{j}{n}\right) \frac{e^2 N_A}{4\pi\epsilon_0\epsilon_r d} \frac{e^{\kappa(a-r_{ij})}}{\left(\frac{r_{ij}}{d}\right)(1+\kappa a)} = \frac{e^2 N_A ij}{4\pi\epsilon_0\epsilon_r d} \frac{1}{pn} \sum_{i,j} \frac{e^{\kappa(a-r_{ij})}}{\left(\frac{r_{ij}}{d}\right)(1+\kappa a)} = \frac{e^2 N_A ij}{4\pi\epsilon_0\epsilon_r d} H_{pn} \quad \text{(A10)}$$

with

$$H_{pn} = \frac{1}{pn} \sum_{i,j} \frac{e^{\kappa(a-r_{ij})}}{\left(\frac{r_{ij}}{d}\right)(1+\kappa a)} \quad \text{and}$$

$$r_{ij} = (R_n^2 + R_p^2 + d^2 - 2\cos\theta_{ij}')^{1/2} \quad \text{(A11)}$$

where d designates the distance between the centers of the parallel circular distributions of positive and negative charges and θ'_{ij} is the dihedral angle between the vectors $\overrightarrow{O_p i}$ and $\overrightarrow{O_n j}$ (Figure 3). H_{pn} is a function of R_n, R_p, d, n, p, κ^{-1}, a, and, a priori, θ_0, a reference dihedral angle providing the relative angular position of both polygonal distributions of charges in interaction (Figure 3). We have confirmed that H_{pn} does not depend on θ_0 when p and n are as large as in the present case ($n = 7$ and $p = 6$, 7, or 8). The H_{pn} function was then studied by using the R_n and R_p values obtained from the analysis of the proton dissociation constants according to the most reliable model D and by taking $d = 0.6$ nm as suggested by the previous NMR investigation.[4] In view of the observed discrepancy for CD7(Ac), the radius of CD7(Am) has been adopted for both the β-cyclodextrin derivatives. Like G_n, H_{pn} exhibits a two-regime dependence on κ^{-1} (Figure 5Sa). For the lowest values of κ^{-1}, H_{pn} is logarithmically dependent on κ^{-1}, whereas it levels off at large κ^{-1} values. This observation is in line with the κ^{-1}-scaled screening effect. More (i, j) couples become available for electrostatic interaction when κ^{-1} is increased. When κ^{-1} overcomes the largest distance r_{ij}, all the couples (i, j) governing the electrostatic interaction are taken into account and H_{pn} essentially does not change anymore. It is interesting to notice that the H_{pn} function does not considerably depend on the p values. Hence, the theory suggests the three examined CD-*p*(Am):CD*n*(Ac) couples to exhibit very similar linear $\Delta_r G^0_{ij}(ij)$ relationships. Figure 5Sb displays the predicted slope S_{pn} of the $\Delta_r G^0_{ij}(ij)$ linear function.

Model C. The W^0_ν terms corresponding to the electrostatic works for charging the individual cyclodextrin species are the same as for model B. Moreover, $\Delta_r G^0_\nu$ now contains an additional term of configurational entropy. Equation 6 becomes

$$\Delta G^0_\nu = W^0_\nu - RT \ln \Omega_\nu = W^0_\nu - RT \ln\left[\frac{n!}{\nu!(n-\nu)!}\right] \quad \text{(A12)}$$

and eqs 10 and 11 now provide

CD*p*(Am) series:

$$pK_a(x) - \frac{\ln\left(\frac{x}{p+1-x}\right)}{\ln 10} = pK_{int}(Am) - \frac{N_A e^2 (1+2p) G_p}{8\pi\epsilon_0\epsilon_r RT \ln 10 R_p} + \frac{N_A e^2 G_p}{4\pi\epsilon_0\epsilon_r RT \ln 10 R_p}(x) \quad \text{(A13.a)}$$

CD*n*(Ac) series:

$$pK_a(x) - \frac{\ln\left(\frac{x}{n+1-x}\right)}{\ln 10} = pK_{int}(Ac) - \frac{N_A e^2 G_n}{8\pi\epsilon_0\epsilon_r RT \ln 10 R_n} + \frac{N_A e^2 G_n}{4\pi\epsilon_0\epsilon_r RT \ln 10 R_n}(x) \quad \text{(A13.b)}$$

Model D. The $W^{0(k)}_\nu$ and $\Omega^{(k)}_\nu$ are calculated according to Tanford and Kirkwood.[10] $W^{0(k)}_\nu$ can be expressed as a linear combination $\sum_k (1/2) c_k \varphi_k$ of three ($p = 6$ or 7) or four ($p = 8$) pairwise interaction energies φ_k. φ_k is the electrostatic energy of a pair of charges that are separated by ($k - 1$) corners along the polygon rim (Figure 2). It is expressed by

$$\varphi_k = \frac{N_A e^2 e^{\kappa(a - R_n[2(1-\cos\theta_{ij})]^{1/2})}}{4\pi\epsilon_0\epsilon_r R_n [2(1-\cos\theta_{ij})]^{1/2}(1+\kappa a)} \quad \text{(A14)}$$

where θ_{ij} designates the angle between the segments originating from the polygon center and respectively linked to i and j (Figure 2). The tables giving $W^{0(k)}_\nu$ and $\Omega^{(k)}_\nu$ for the different configurations (ν, k) in the three symmetry groups D_{6h}, D_{7h}, and D_{8h} are given in the Supporting Information. They directly apply to the series of cyclodextrin amines. In the series of cyclodextrins bearing carboxylic acid groups, the occupation of a corner site by a proton removes one charge to the CD backbone, and the preceding tables remain valid by transforming ν into $n + 1 - \nu$.

Supporting Information Available: The experimental titration curves, the analysis of the numerical factors G_n, H_{pn}, and S_{pn}, the appropriate charging works and degeneracies under application of the model D, an example of a phase diagram for electrostatic interaction (22 pages). See any current masthead page for access and ordering information.

References and Notes

(1) Conn, M. M.; Rebek, J. *Chem. Rev.* **1997**, *97*, 1647.
(2) Guillo, F.; Jullien, L.; Hamelin, B.; Lehn, J.-M.; De Robertis, L.; Driguez, H. *Bull. Soc. Chim. Fr.* **1995**, *132*, 857.

(3) Hamelin, B.; Jullien, L.; Guillo, F.; Lehn, J.-M.; Jardy, A.; De Robertis, L.; Driguez, H. *J. Phys. Chem.* **1995**, *99*, 17877.

(4) Hamelin, B.; Jullien, L.; Derouet, C.; Hervé Du Penhoat, C.; Berthault, P. *J. Am. Chem. Soc.* **1998**, *120*, 8438.

(5) Hamelin, B.; Jullien, L. *J. Chem. Soc., Faraday Trans.* **1997**, *93*, 2153.

(6) Mammen, M.; Simanek, E. E.; Whitesides, G. M. *J. Am. Chem. Soc.* **1996**, *118*, 12614. Mammen, M.; Shahnovich, E. I.; Deutch, J. M.; Whitesides, G. M. *J. Org. Chem.* **1998**, *63*, 3821.

(7) Israelachivili, J. *Intermolecular and Surface Forces*, 2nd ed.; Academic Press: London, San Diego, New York, Boston, Sydney, Tokyo, Toronto, 1991. Gerschel, A. *Liaisons intermoléculaires*; InterEditions et CNRS Editions: Paris; 1995.

(8) In fact the thermodynamic constant P_k for the chemical process 2 is expressed by the relation

$$-RT \ln P_k = -RT \ln \left[\sum_{\substack{(i,j) \\ i-j=k-7}} \exp\left(-\frac{\Delta_r G^0_{ij,k}}{RT} \right) \right]$$

where the $\Delta_r G^0_{ij,k}$ designate the standard Gibbs free energies of the different chemical processes 2. In principle, the derivation of the standard Gibbs free energies of the chemical processes 3, $\Delta_r G^0_{ij}$, from P_k would thus require one to take into account several couples (i, j) fulfilling the condition $i - j = k - 7$, that is, $(\sup\{i\}, \sup\{j\})$, $(\sup\{i\} - 1, \sup\{j\} - 1)$, ... As will be shown later, one experimentally observes the linear relationship $-\Delta_r G^0_{ij}$ (kJ·mol^{-1}) $= 12.4 + 0.85ij$. Then the respective contributions of two successive $\Delta_r G^0_{ij,k}$ terms in the P_k expression can be evaluated

$$\exp\left(-\frac{\Delta_r G^0_{(i-1)(j-1)} - \Delta_r G^0_{ij}}{RT} \right) = \exp\left(\frac{0.85(1 - i - j)}{RT} \right) \approx 0.05 \ll 1$$

with $T = 298$ K and $i = j = 5$ to derive a typical order of magnitude. Hence, it appears reasonable to retain the largest term $\Delta_r G^0_{\sup\{i\}\sup\{j\}}$ in a first approximation so as to assume $-RT \ln P_k = \Delta_r G^0_{\sup\{i\}\sup\{j\}}$ with $i - j = k - 7$. Then P_k is identified as P_{ij}, whereas $\Delta_r G^0_{\sup\{i\}\sup\{j\}}$ simply gives $\Delta_r G^0_{ij}$.

(9) Schafer, M.; Sommer, M.; Karplus, M. *J. Phys. Chem. B* **1997**, *101*, 1663 and references therein.

(10) Tanford, C.; Kirkwood, J. G. *J. Am. Chem. Soc.* **1957**, *79*, 5333. Tanford, C. *J. Am. Chem. Soc.* **1957**, *79*, 5340.

(11) The approach used in ref 10 was essentially retained in this paragraph. Like in ref 10, the reference system is the infinitely diluted solution at zero ionic strength parametered by the molar concentrations (standard concentration 1 M). As usual, the exponent ^{0} is used to designate standard functions ($\Delta_r G°$, W^0, ...).

(12) In the present system, the structural investigation reported in ref 4 suggests this assumption to be reasonable.

(13) A less sophisticated model was used in our preliminary report.[3] At that time, the cyclodextrin backbone was simply modeled as a sphere.

(14) In the previous report,[3] the reference system was taken as the infinitely diluted solution at the ionic strength that was used during the potentiometric titration. Thus the activity coefficients were only measuring the interaction between the (diluted) cyclodextrin species. In the present case, the activity coefficient expresses the interaction of the cyclodextrin species with all the species present in solution.

(15) Bockris, J. O'M.; Reddy, A. K. N. In *Modern Electrochemistry*, 6th ed.; Plenum Press: New York, 1977.

(16) See ref 10 for taking into account a discontinuity of the dielectric constant.

(17) See ref 15, T1, p 156.

(18) See ref 15, T1, p 157.

(19) The present study can be used to examine the significance of the discreteness of the solvent structure for rationalizing the acid−base and association features of objects such as the derivatized cyclodextrins reported herein. In fact, the cyclodextrin series is especially suitable for such a purpose since the backbones of the α-γ-cyclodextrins have diameters ideally lying within a few diameters of the water molecule. This system is thus prone to reveal the significance of symmetry or scale factors for affecting interaction properties in such a locally structured medium as liquid water (the role of the local symmetry of water clusters with regard to the cyclodextrin symmetry was already evoked for accounting for the behavior of a series of amphiphilic cyclodextrins at the air−water interface (see: Schalchli, A.; Benattar, J. J.; Tchoreloff, P.; Zhang, P.; Coleman, A. W. *Langmuir* **1993**, *9*, 1968)). No singular behavior of acid−base properties revealing the role of scale or symmetry has been observed in the CD*p*(Am) series. Thus the intrinsic pK_{int} for the three investigated CD*p*(Am) were found equal (see Table 3). On the basis of the identical molecular structure and environment of each glucose unit in the CD*p*(Am) series, such a result points out that the solvation of the opposite side of the CD primary rim does not considerably affect the primary solvation shell of given amino groups. Moreover, models C and D provide consistent structural results without special adjusment for any particular CD*p*(Am) derivative. Hence, these results suggest the medium description as a continuum to be appropriate at the nanometer scale for evaluating the charge−charge interaction in the present system. The same conclusion arises from the investigation of the associative properties between the different series of oppositely charged cyclodextrins. The similar behaviors of the three investigated couples conform to the theoretical expectations predicted by model B/C without introducing any scale- or symmetry-dependent factor.

(20) The charge−charge distance within each CD unit is about 1 nm, whereas the previous structural investigation[4] demonstrated the distance *d* between oppositely charged CD to be about 0.6 nm. Both characteristic distances lie above a few diameters of the water molecule. Thus it seems reasonable that the detailed structure of the solvent can be ignored in the present system. At shorter characteristic distances that directly concern the primary solvation shells, scale or symmetry factors could be more prone to manifest themselves.

(21) Lipkowitz, K. B.; Green, K.; Yang, J. *Chirality* **1992**, *4*, 205.

(22) Brown, S.; Coates, J. H.; Coghlan, D. R.; Easton, C. J.; van Eyk, S. J.; Janowski, W.; Lepore, A.; Lincoln, S. F.; Luo, Y. *Aust. J. Chem.* **1993**, *46*, 953.

(23) Szejtli, J. *Chem. Rev.* **1998**, *98*, 1743.

(24) It is possible that the extracted radii for the β- and γ-derivative are slightly overestimated owing to too low an ϵ_r value for the R_{CD} evaluation. In fact, the theoretical treatments developed in the Appendix only provide the product of the effective dielectric constant by a characteristic size (see Table 3). As explained above, we decided to keep ϵ_r equal to 50 during this investigation. In fact, one a priori expects the relevant value of the effective ϵ_r to increase when the cyclodextrin diameter increases, that is, ϵ_r(α-CD) < ϵ_r(β-CD) < ϵ_r(γ-CD). Indeed the local concentration of ions drops and the surrounding water molecules become more bulklike when going from the α- to the γ-CD series. By taking $\epsilon_r = 60$, the extracted radii decrease by about 15%.

(25) Rouzina, I.; Bloomfield, V. A. *J. Phys. Chem.* **1996**, *100*, 4292. Rouzina, I.; Bloomfield, V. A. *J. Phys. Chem.* **1996**, *100*, 4305. Mohanty, U.; Ninham, B. W.; Oppenheim, I. *Proc. Natl. Acad. Sci. U.S.A.* **1996**, *93*, 4342.

(26) This explains why we correlated $\Delta_r G^0_{ij}$ with *ij* instead of correlating $\Delta_r G^0_{ij}$ with some other parameter like *i* that would evaluate the number of pairs of closest interacting opposite charges when $i = j$. See, for instance: Schneider, H.-J. *Angew. Chem., Int. Ed. Engl.* **1991**, *30*, 1417. Schneider, H.-J. *Chem. Soc. Rev.* **1994**, 227 and references therein.

(27) Rosset, R.; Bauer, D.; Desbarres, J. In *Chimie analytique des solutions et informatique*; Masson: Paris, Milan, Barcelone, Bonn, 1991.

(28) Linderström-Lang, K. *Compt. Rend. Trav. Lab. Carlsberg* **1924**, *15*, 7.